The Continuous Measurement of the Damping and Fatigue Properties of High-Impact Polystyrene with a Controlled-Amplitude Torsion Pendulum.

H. BARTESCH and D. R. G. WILLIAMS, *Chemical Engineering Department (Materials Engineering), University of Adelaide, Adelaide, South Australia*

Synopsis

Torsional damping and fatigue studies were made on high-impact polystyrene using a controlled-amplitude, continuously recording torsion pendulum. The damping behavior was measured as a function of the angular displacement, axial tensile stress, and the number of repeated cycles. At a critical axial tensile stress, the damping behavior changed from amplitude-independent to amplitude-dependent behavior. Damping measurements on high-impact polystyrene specimens that had been previously crazed in tension showed that both the damping and the tensile stress necessary to produce amplitude-dependent damping varied with the orientation of the craze. Repeated cycling of HIPS specimens produced crazing and amplitude-dependent damping at a tensile stress below that expected from simple static tensile loading. Scanning electron micrographs of fracture surfaces from these specimens revealed that the rubber particles could be clearly distinguished from the surrounding matrix.

INTRODUCTION

The measurement of the damping properties of polymers is a valuable technique to ascertain the mobility of various structural units in the constitution of polymers. The techniques normally adopted involved the application of low oscillating stresses at frequencies above approximately 1 Hz, and under these conditions the specimen behavior can usually be described by linear viscoelastic theory where the derived damping parameter is assumed to be independent of amplitude. Indeed, the experimental determination of the damping parameter by methods such as free decay of oscillations or the measurement of resonance peaks does not allow the unambiguous interpretation of the effect of variation in amplitude. If the amplitude is controlled and the energy loss per cycle measured, then nonlinear viscoelastic behavior can be examined.

A particular deformation mode of polymers that is of current interest and is known[1] to exhibit nonlinear viscoelastic behavior is crazing. The process of crazing has been extensively investigated,[2,3] but there remains an area of uncertainty surrounding the mechanical behavior of the craze material itself. For example, the crazing of either clear polystyrene or high-impact polystyrene ($T_g \simeq 100°C$) at room temperature implies that considerable chain mobility must occur, the craze material being generally understood to consist of orientated polymer chains plus voids. Furthermore, this craze material can exhibit recovery[4,5] at temperatures far removed from the glass transition temperature.

The objective of this work was to examine the damping behavior of polymers

Journal of Applied Polymer Science, Vol. 22, 467–486 (1978)

0021-8995/78/0022-0467$01.00

at sufficiently high tensile stresses to induce crazing and to use the same technique to investigate the early stages of fatigue.

EXPERIMENTAL

The most satisfactory method to follow the damping and fatigue behavior of polymers during crazing was to use an inverted torsion pendulum capable of maintaining angular deflections at set amplitudes. Tensile stresses could be superimposed to either induce crazing in situ or to produce tensile strains in already crazed specimens.

The conventional method of measuring the damping with a torsional pendulum is from the logarithmic decay of oscillations and is not appropriate in this case. To maintain a set amplitude of oscillation, an electromagnetic drive was used, and the energy loss per cycle, ΔE, was calculated from the equation

$$\Delta E = \frac{8}{\pi} I_1 I_2 \theta_{\max} K \tag{1}$$

where I_1 = peak current in the field coil, I_2 = current in the driven coil, $\theta_{\max}$ = peak angular deflection, and

$$K = \frac{N_1 N_2 \mu_0 l r}{g} \tag{2}$$

where N_1 = number of wire turns in the field coil, N_2 = number of wire turns in the driven coil, μ_0 = reluctance of air, g = width of the air gap, r = middle radius of the air gap, and l = height of the field coil.

To verify the value of ΔE obtained from eq. (1), the logarithmic decrement Δ was calculated from the equation

$$\Delta = \tfrac{1}{2} \frac{\Delta E}{E} \tag{3}$$

and the value compared to the logarithmic decrement obtained from free decay measurements using the equation

$$\Delta = \ln \frac{\theta_1}{\theta_2} \tag{4}$$

where θ_1 and θ_2 are the amplitudes of successive swings.

The logarithmic decrement from constant amplitude measurements was determined for low angular displacements and low tensile stresses using materials that were known to possess amplitude-independent behavior. The stored energy

TABLE I
Comparison of Logarithmic Decrements

Material	Δ from free decay, eq. (4)	Δ from energy loss, eq. (8)
Polystyrene	0.0414	0.0420
Poly(methyl methacralate)	0.0514	0.0516
HIPS	0.0540	0.0545

E was determined under static conditions for the same angular displacement θ_{max} and is given by

$$E = \tfrac{1}{2}D\theta^2_{max} \tag{5}$$

where D, a material constant, is determined from the torque T by the relation

$$D = T/\theta_{max} \tag{6}$$

The static torque T required to produce an angular deflection θ_{max} is given by

$$T = KI_1'I_2' \tag{7}$$

where I_1' and I_2' are the dc currents in the coils. Combining eqs. (3), (5), (6), and (7) gives

$$\Delta \text{ (from energy loss)} = \frac{8}{\pi}\frac{I_1I_2}{I_1'I_2'} \tag{8}$$

Comparison of values of Δ obtained directly from free decay and values of Δ derived from energy loss measurements are listed in Table I. The values differ by less than 1%.

Further information on the performance and accuracy of the controlled-amplitude torsion pendulum is given elsewhere.[7]

The energy loss data could be collected for each cycle, and the average value of ten cycles was transferred to punch tape for processing by computer. The frequency of oscillation was approximately 1 Hz. All damping measurements were made at 30°C.

The motor could be operated statically with constant currents applied to produce a particular torque. Angular deflections were measured with a Sefram Photodyne lightspot recorder. Calibration was achieved by counterbalancing the applied torque with weights. The relationship between applied torque and applied current was linear up to a torque of 0.25 Nm.

For the fatigue tests, initially uncrazed specimens were cycled at a constant amplitude of 0.1 rad and subjected to a tensile stress σ_v = 11 MPa. This value of the tensile stress was chosen to be below that stress which was capable of inducing crazing during a normal energy loss determination as described previously. After a number of repeated cycles, the energy loss was measured throughout the torsional amplitude range of 0–0.1 rad.

In order to maintain a constant recovery period, all tensile tests on the precrazed specimens were carried out 24 hr after the initial induction of crazing. The effect of variation in the strain rate was measured on uncrazed HIPS specimens.

Material

A sheet of high-impact polystyrene (Monsanto: LUSTRUX Grade B10-4) 3.9 × 200 × 200 mm was produced by compression molding. "Uncrazed" samples were cut from this sheet and milled to size (3.9 × 8 × 100 mm). To obtain "precrazed" specimens, the complete sheet was strained at a cross-head speed of 50 mm/min until an extensive uniform area of crazing appeared over most of the sheet (ϵ = 5%). Precrazed specimens were then cut from this sheet at 0°, 45°, and 90° to give specimens with crazes perpendicular, 45° diagonal, and parallel

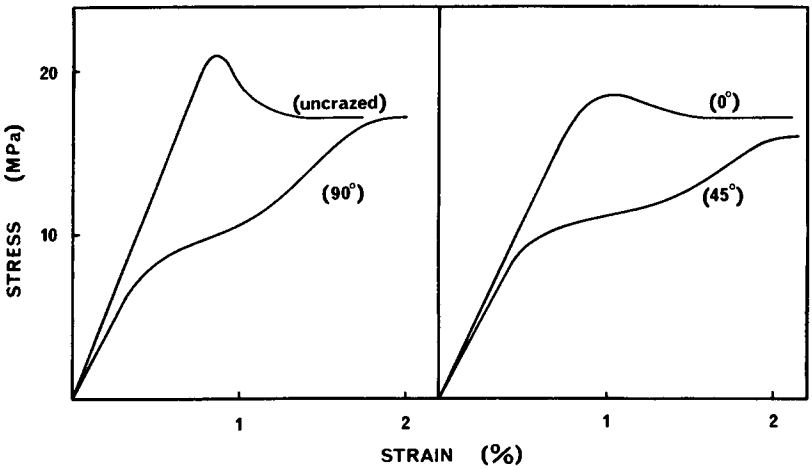

Fig. 1. Tensile stress–strain results for uncrazed HIPS and 0°, 45°, and 90° precrazed HIPS.

to the longitudinal axis of the specimen; these specimens shall be referred to as 0°, 45°, and 90° precrazed specimens.

RESULTS

Tensile Tests

The stress–strain results for the uncrazed and precrazed HIPS specimens are presented in Figure 1. The values of the initial modulus E, yield stress σ_Y, and drawing stress σ_D are presented in Table II. The additional subscripts refer to the uncrazed (virgin) material (1) and precrazed material (2). (By referring to σ_{Y2} for the precrazed specimens, it is, therefore, acknowledged that these specimens have already undergone a stress–strain cycle to produce crazing.) The yield stress is defined as that stress at which the curve first departs from linearity, and the drawing stress is defined as the stress asymptotically approached at large strains.

Cycling

A procedure similar to that of Bucknall[17] was used to observe the behavior of HIPS subject to an oscillating load. The specimen was loaded until the drawing stress was reached and then returned to zero load; this cycle was repeated. The

TABLE II
Modulus, Yield Stress, and Drawing Stress of Uncrazed and Precrazed HIPS

	E_1, GPa	E_2 GPa	σ_{Y1}, MPa	σ_{Y2}, MPa	σ_D, MPa
Uncrazed	2.0		21.0		17.2
Precrazed					
0°		2.0		17.1	17.1
45°		1.9		8.3	16.3
90°		1.8		6.3	17.2

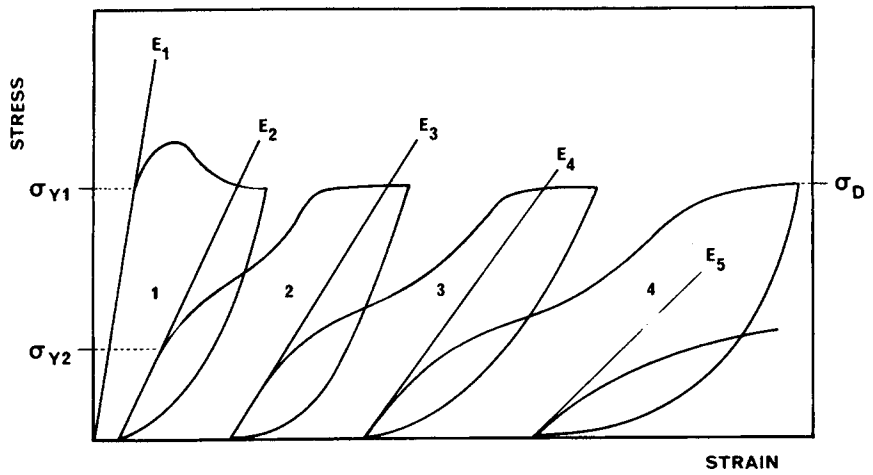

Fig. 2. Nominal tensile stress–engineering strain curves for HIPS repeatedly loaded and unloaded.

results for the particular grade of HIPS used in this investigation are plotted in Figure 2 as the nominal stress versus the engineering strain. In particular, we wish to specify on these curves the initial yield stress for the first cycle σ_{Y1}, the yield stress for successive cycles $\sigma_{Y2}, \sigma_{Y3} \ldots$, the drawing stress σ_D, and the initial moduli for successive cycles $E_1, E_2, E_3 \ldots$.

On the first cycle, the mechanism of deformation involves the initiation of crazes at a stress close to the point where the curve departs from linearity. With further crazing, a strain softening phenomenon occurs and the stress drops to a constant value called the drawing stress σ_D. Crazes initiated will continue to grow at this stress level until the stress is removed. On removal of the load, the crazes will partially collapse under the constraint of the surrounding glassy matrix and will begin the process of recovery.[4,5] On reloading, a new yield stress σ_{Y2} is observed followed by a reopening of the crazes. Considerable strain hardening occurs on the approach to stress level σ_D. It is suggested that the strain hardening process may involve a component associated with normal orientation hardening of the craze material plus a component associated with the restricted deformation of the rubber particles under the hydrostatic tensile conditions. At the drawing stress level, further crazes will not be initiated as remaining glassy material is required to sustain a higher load.

Calculation of the relative cross-sectional area of the crazes and the remaining polystyrene matrix can be made from the values of the initial moduli. Assuming that HIPS can be considered after the first cycle as a composite material consisting of crazes imbedded in a polystyrene matrix, then the total load on the specimen is shared by the crazes and the polystyrene matrix:

$$P_T = P_C + P_G$$

and

$$\sigma_T A_T = \sigma_C A_C + \sigma_G A_G$$

where σ_T, σ_C, and σ_G are the stresses caused on the total specimen, craze, and

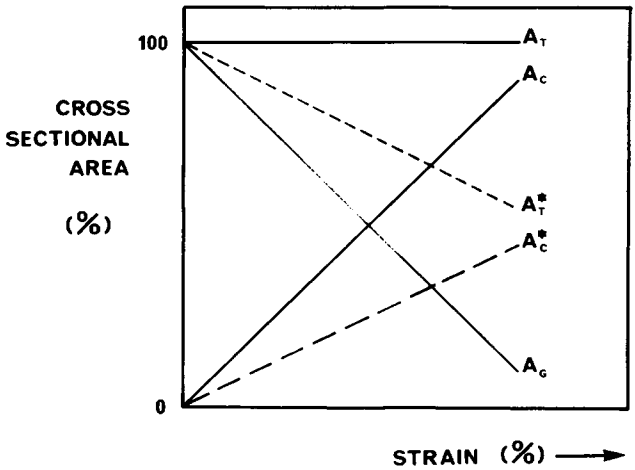

Fig. 3. Schematic diagram of the relative changes in areas of material during straining of HIPS.

glass, respectively; and A_T, A_C, and A_G are the respective cross-sectional areas of the total specimen, craze, and glass.
Substituting $\sigma = E\epsilon$

$$E_T\epsilon_T A_T = E_C\epsilon_C A_C + E_G\epsilon_G A_G \tag{9}$$

where E_T, E_C, E_G and ϵ_T, ϵ_C, ϵ_G are the respective moduli and strain of the specimen, craze, and glass.

Now it has been suggested by several authors[2–4] that, on unloading from σ_D on the first cycle, the crazes will partially collapse under the constraint of the elastic relaxation of the surrounding glassy matrix. If reloading is commenced immediately, then only a relatively small degree of recovery will have occurred, and it can be assumed that until ϵ_1 is reached, the modulus E_C of the craze will be approximately zero. That is, the composite will initially act as a glassy polymer with a reduced cross-sectional area. Therefore, from eq. (9), the remaining cross-sectional area of the glassy polymer is given by

$$A_G = \frac{E_T}{E_G}$$

By substituting $E_2 = E_T$ and $E_1 = E_G$, the value of the cross-sectional area of glass and craze can be determined. This process can be continued for further

TABLE III
Relative Areas of Craze and Glass

Strain, %	A_C	A_G
0	0	100%
2	12	88
4	32	68
6	60	40
8	~65	~35

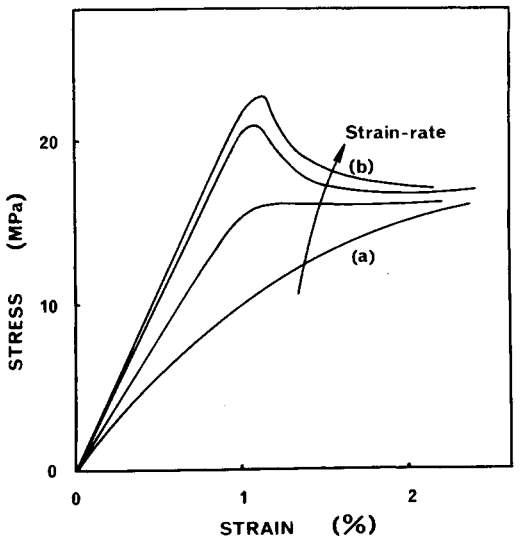

Fig. 4. Stress–strain curves for uncrazed HIPS specimens at strain rates from (a) 5×10^{-3} min^{-1} to (b) 5 min^{-1}.

cycles until the initial moduli, for example, E_5, become difficult to determine accurately. The results are presented in Table III.

It has been shown[3] that a craze consists of 40–60% of voids. It is assumed that if the active craze area $A_C = 0.5A_C$, then a schematic plot of the relative areas as the strain increases at the drawing stress can be plotted as in Figure 3. Thus, the total active area consisting of active craze material and glassy matrix continues to decrease. Therefore, although the nominal drawing stress remains constant, the true drawing stress will increase, allowing the initiation of crazes at smaller rubber particles.

Strain Rate

The effect of increasing the tensile strain rate on initially uncrazed specimens was to encourage the formation of a response which exhibited pronounced strain softening (Fig. 4). The amount of strain softening can be defined as the difference between the maximum recorded tensile stress and the drawing stress σ_D, calculated as a percentage of σ_D. At a slow strain rate of 5×10^{-3} per min, the strain softening was 16%; and for a high strain rate of 5 per min, the strain softening was 70%. As discussed by Bucknall,[17] the maximum tensile stress is reached when the initiation and growth rate of crazes match the strain rate. After this point, the stress drops to the drawing stress, and further growth and initiation of crazes can occur at the lower drawing stress level. As observed by Sauer et al.[9] and also in the current experiments, the density of crazes increases with increases in strain rate.

From examination of thin sections, Stabenow[10] was able to show that large rubber particles were able to induce crazing at lower stress levels and that higher stress levels were required to initiate crazes at smaller rubber particles. The results are consistent with the view that at high strain rates, a larger size range

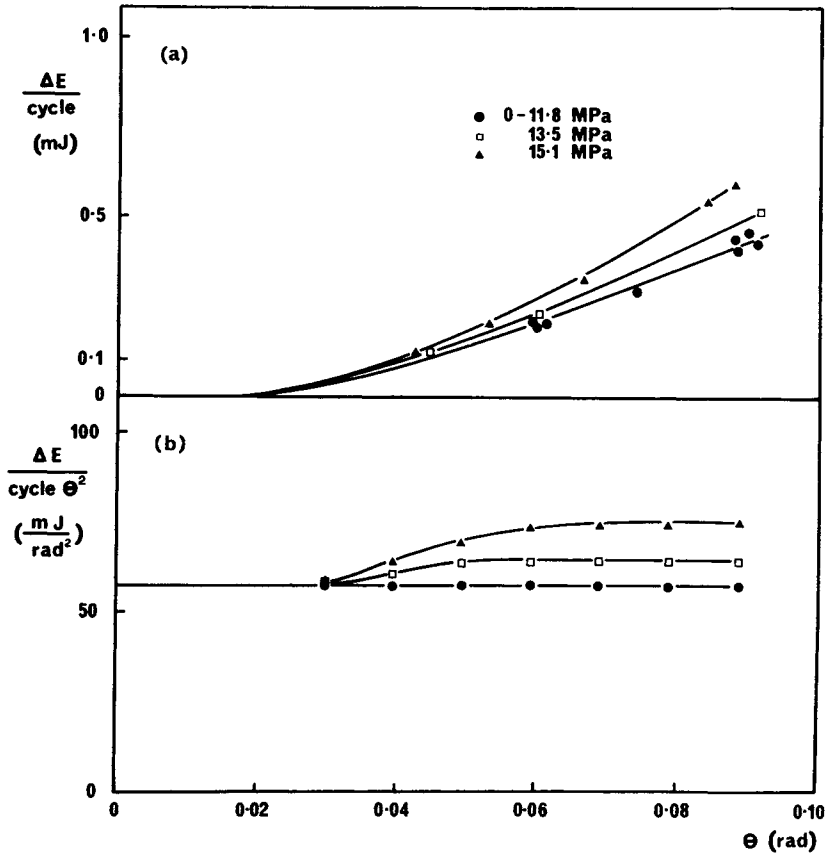

Fig. 5. (a) Energy loss ΔE per cycle of uncrazed HIPs as a function of the amplitude and (b) the energy loss per cycle per θ^2 as a function of the amplitude, subjected to various tensile stresses σ_b.

of rubber particles will be involved to produce a higher craze density and, therefore, a higher percentage of strain softening.

Damping Behavior of HIPS

The results of the damping experiments can be plotted as the energy loss ΔE per cycle versus the angular deflection for different applied tensile stresses. For example, Figure 5(a) shows the results for an initially uncrazed specimen of HIPS where the ordinate parameter represents the absolute energy loss per cycle. Now eq. (5) can be generalized[11] to give

$$\Delta E = D' \theta_{\max}^{m}$$

where D' is a material constant, $\theta_{\max}$ is the maximum angle of deflection, and m is the damping exponent. If the behavior of the material dissipating energy can be described by linear viscoelastic models, then the damping is logarithmic (i.e., amplitude independent) and the exponent will have the value of $m = 2$. So it is appropriate to replot the results as the energy dissipated per cycle per square of the maximum angular deflection as in Figure 5(b). A positive slope of the curve ($m > 2$) will, therefore, indicate that the material must be behaving in a

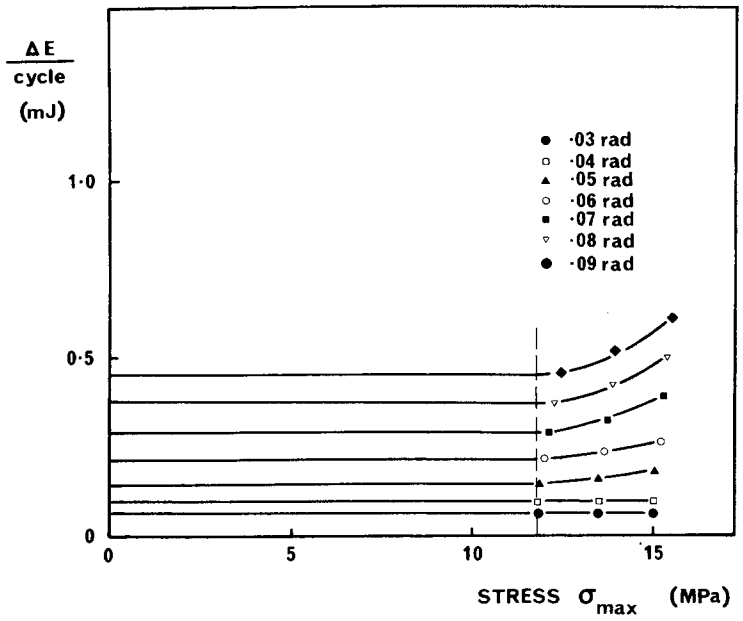

Fig. 6. Energy loss ΔE per cycle as a function of the maximum stress for uncrazed HIPS.

nonlinear viscoelastic manner and that the damping can be described as nonlogarithmic and amplitude dependent.

The results can also be presented in a third form where the energy loss per cycle is plotted versus the maximum tensile stress, σ_{max} for various angles of deflection (Fig. 6). The maximum tensile stress is calculated as the sum of the vertically applied tensile stress plus the tensile component resulting from the torsional deflection.

Uncrazed HIPS

It can be seen from Figure 5(b) that the damping behavior remains amplitude independent at all angular deflection until the applied tensile stress reaches a value of approximately 11.8 MPa. At this stress, a marked change occurred in the opaqueness of the specimen that indicated the appearance of crazes.

At high levels of applied stress, the damping behavior become amplitude dependent for angular deflections within a transition zone commencing at $\theta \simeq 0.03$ rad. At higher angular deflection after the transition zone, amplitude-independent damping was again resumed.

Observation of the constant angular deflection curves in Figure 6 indicates that at any particular angular deflection over 0.03 rad, there exists a minimum applied tensile stress above which the damping per cycle commences to increase.

Precrazed HIPS

The damping behavior for the specimens which have been precrazed with crazes at 0°, 45°, and 90° to the longitudinal axis is given in Figures 7 and 8. While the S-shaped curve in Figure 7 appears to be common, there are some

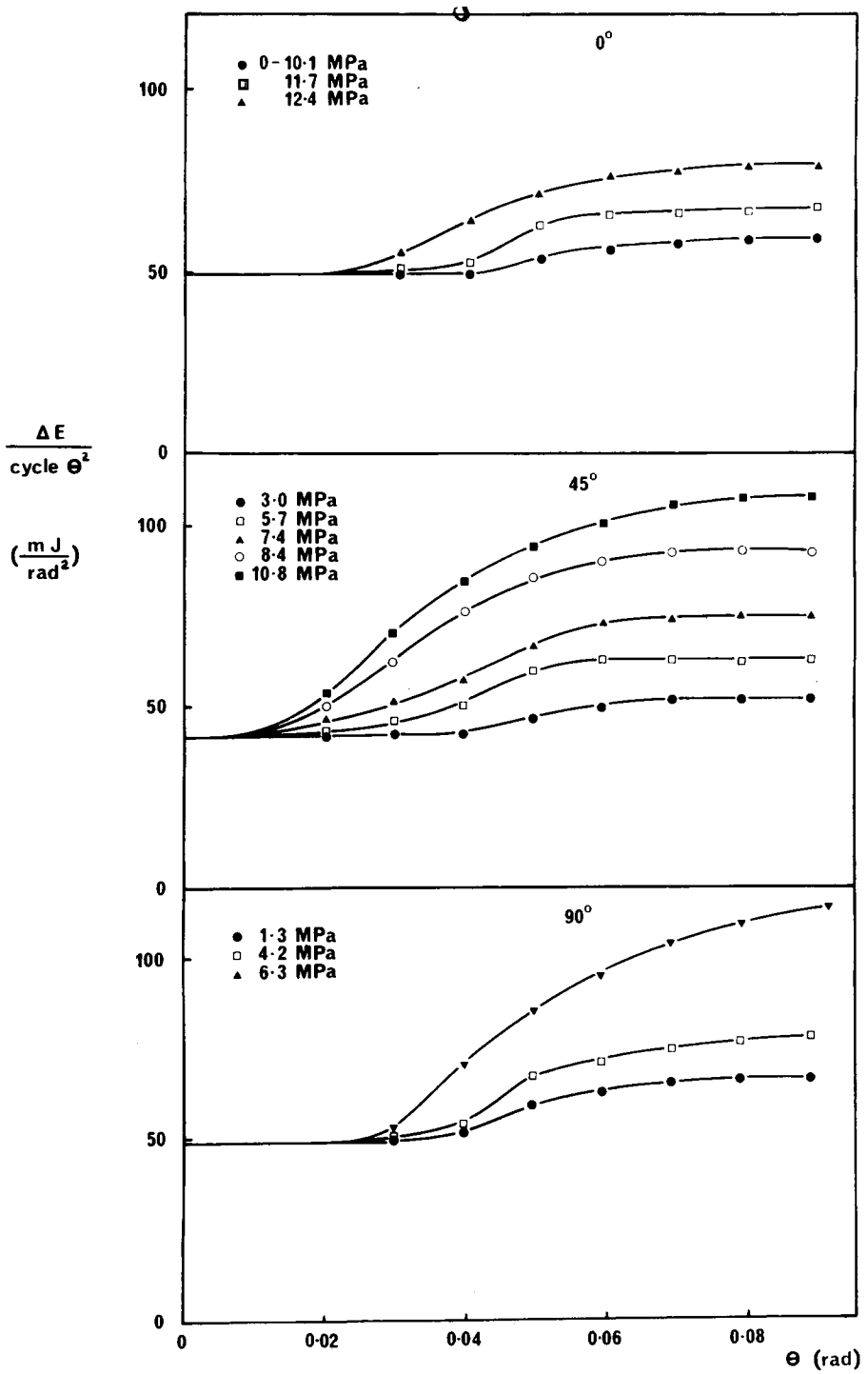

Fig. 7. Energy loss $\Delta E/\theta^2$ per cycle for 0°, 45°, and 90° precrazed HIPS specimens, subjected to various tensile stresses σ_v.

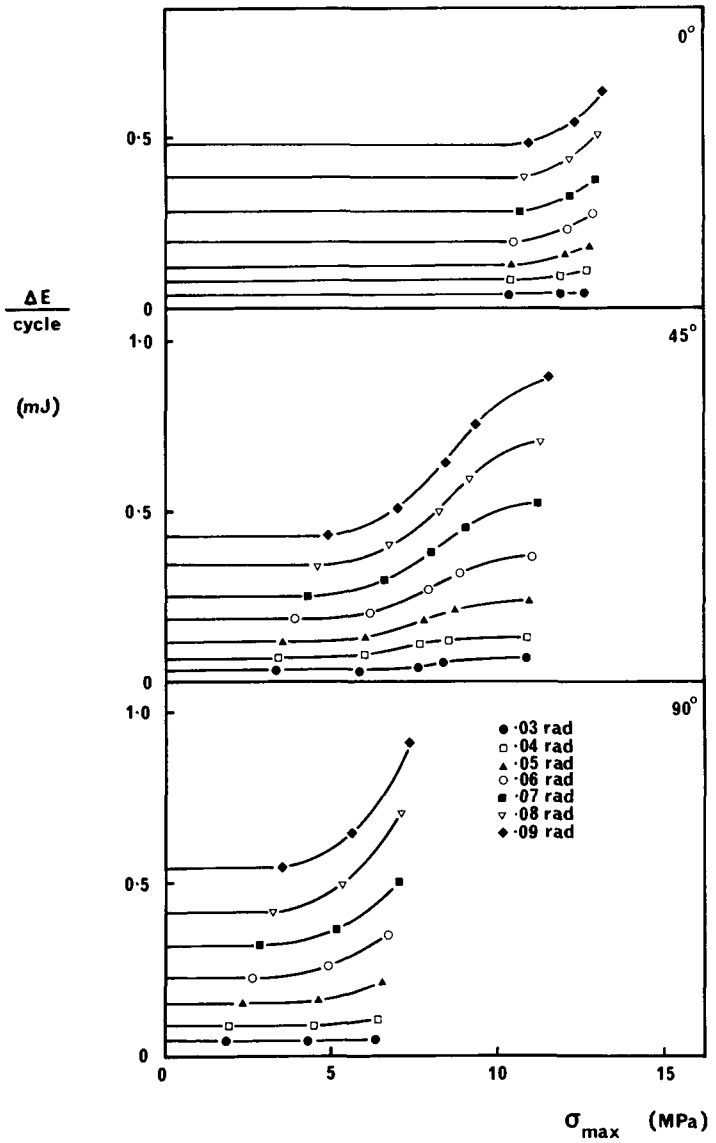

Fig. 8. Energy loss ΔE per cycle as a function of σ_{max} for 0°, 45°, and 90° precrazed HIPS specimens.

notable differences between the specimens. Firstly, amplitude-dependent damping occurs even at low tensile stresses σ_v at angular deflections above 0.03 rad. Secondly, the increase in energy loss $\Delta E/\theta^2$ is more sensitive to the tensile stress σ_v when the crazes are orientated at 90° to the longitudinal axis.

The change in the shear modulus as the tensile stress σ_v is increased (Fig. 9) generally follows a similar behavior to that observed in the tensile stress–strain curves (Fig. 1) for the instantaneous tensile modulus. The specimen that was initially uncrazed and the 0° precrazed specimen show a sudden drop in shear modulus corresponding to the onset of crazing perpendicular to the tensile stress. In comparison, the 45° and 90° precrazed specimens exhibit a decrease in shear modulus at relatively low tensile stress values.

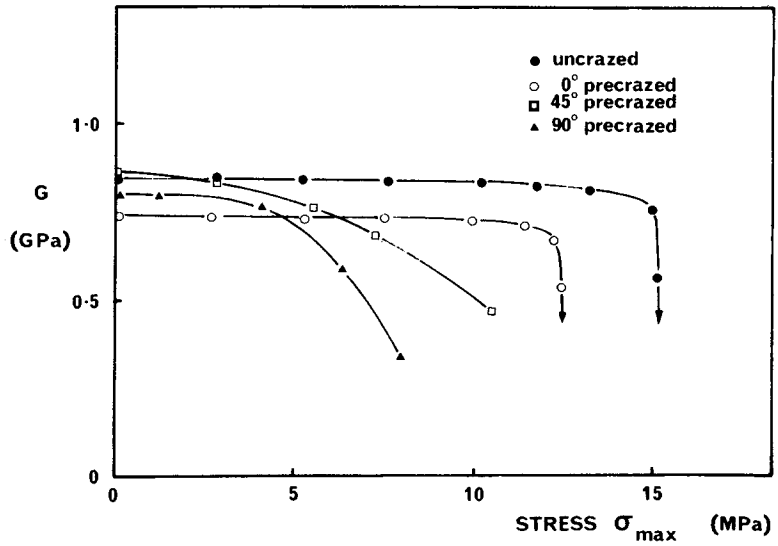

Fig. 9. Shear modulus of uncrazed and crazed HIPS specimens as a function of the applied tensile stress σ_v.

Repeat Cycling

The damping behavior [Fig. 10(a)] and shear moduli [Fig. 10(b)] of initially uncrazed HIPS is presented in a similar manner to the other damping experiments for a tensile stress of σ_v = 11 MPa.

A separate static creep experiment with a stress of 11 MPa revealed no visual indication of crazing for time periods several times those involved in the repeated cycling experiments. This supports the suggestion by Rabinowitz et al.[2] that crazing is induced at lower stresses by cycling than would occur for static fatigue.

Fracture Morphology

Specimens were notched, cooled to liquid nitrogen temperatures, and fractured. The fracture surfaces were coated with gold and examined in the scanning electron microscope.

It was immediately apparent that fracture surfaces which had crazing induced by any form of repeated cycling contained clear evidence of the presence of rubber particles and crazes. The initially uncrazed specimen that had been used in the energy loss determinations and thus subjected to a tensile–shear stress combination, show rubber particles which are clearly distinguishable as spherical areas with fracture surface out-of-plane and exhibiting a different surface texture to the surrounding typically crazed morphology (Fig. 11). By comparison, the fracture surface (Fig. 12) of a specimen subjected to a normal tensile test to failure requires close examination to discriminate between rubber particle and background.

When the torsional oscillations were continued to 16,000 cycles, as in the fatigue experiment, the rubber particles exhibited even further contrast, as shown in the series of photographs in Figure 13 of increasing magnification. Some

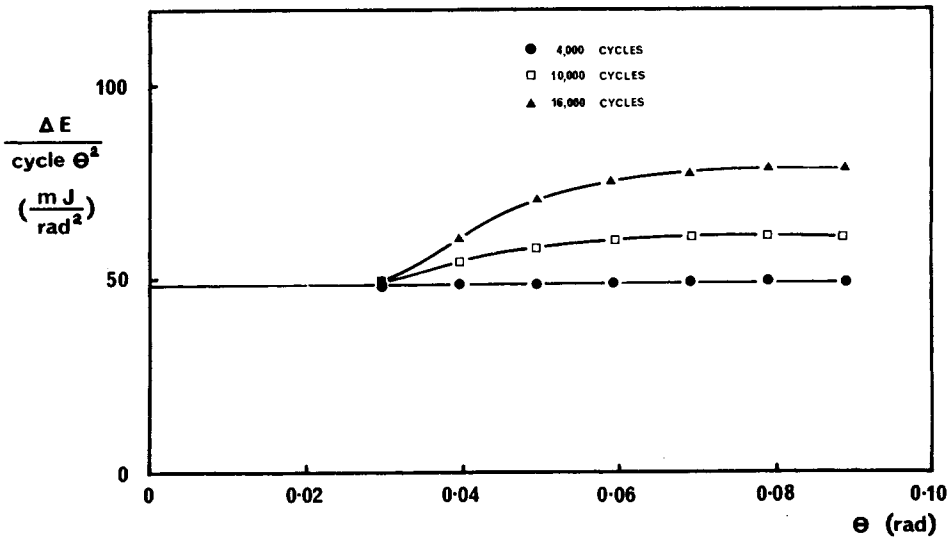

(a)

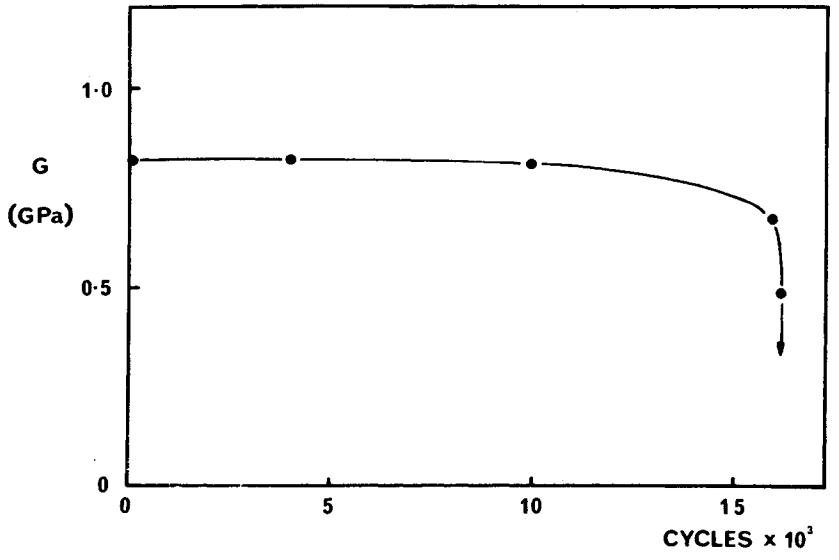

(b)

Fig. 10. Effect of repeated cycling on (a) the energy loss $\Delta E/\theta^2$ per cycle and (b) the shear modulus.

similarity is shown in Figure 13(c) to the results obtained by Manson and Hertzberg[16] for tensile cycled HIPS, but some additional features should be noted. Examination of the cycled specimens suggests that the fracture path passes through the craze and usually through the rubber particles, although in a number of cases the fracture path has gone around the rubber particle [Fig. 13(b)]. In contrast to the numerous sharp facets of the uncrazed specimen [Fig. 12(a)], the fracture path for the cycled specimen is predominately coplanar, with only occasional deviations onto another craze plane.

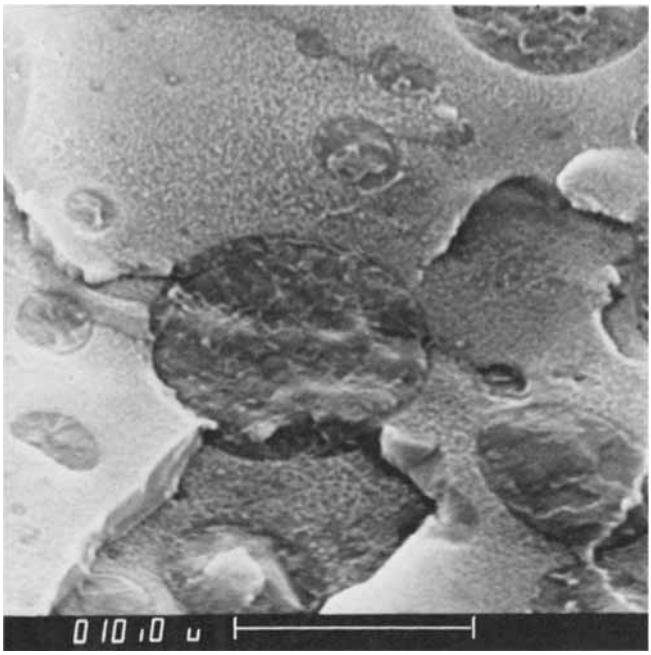

Fig. 11. Typical fracture surface of HIPS specimens from low-cycle energy loss determinations.

Also noticeable with the repeated cycled specimen is the sharp delineation of the boundary between the rubber particle and the surrounding crazed material [Fig. 13(b) and 13(c)]. In comparison, a HIPS specimen crazed at medium strain rates (0.5 min^{-1}) in a normal tensile test shows in Figure 12(b) rubber particles with boundaries that are difficult to distinguish. Indeed, except for an indefinite circumferential line, the rubber particle seems to have the same lightly crazed structure as the surrounding glass. In the fatigued specimens, the rubber particles have now adopted an appearance markedly different to the surrounding matrix.

Except for the occasional unfractured rubber particle, the general observation, especially for the fatigued specimens, was that the rubber particle had retracted leaving a crater-like depression. This would follow the accepted behavior of a highly extended craze where the rubber particle becomes elongated into an elliptic shape. Fracture at liquid nitrogen temperature, followed by relaxation at room temperature, leads to the rubber particle retracting back further than the surrounding crazed material.

DISCUSSION

Torsional Damping

To appreciate the changes of energy loss $\Delta E/\theta^2$ with angular deflection curves, it is helpful to refer to the behavior of HIPS specimens during tensile stress-strain experiments. One difficulty in this procedure which must be remembered is that once a specimen has formed crazes, partial recovery will commence imme-

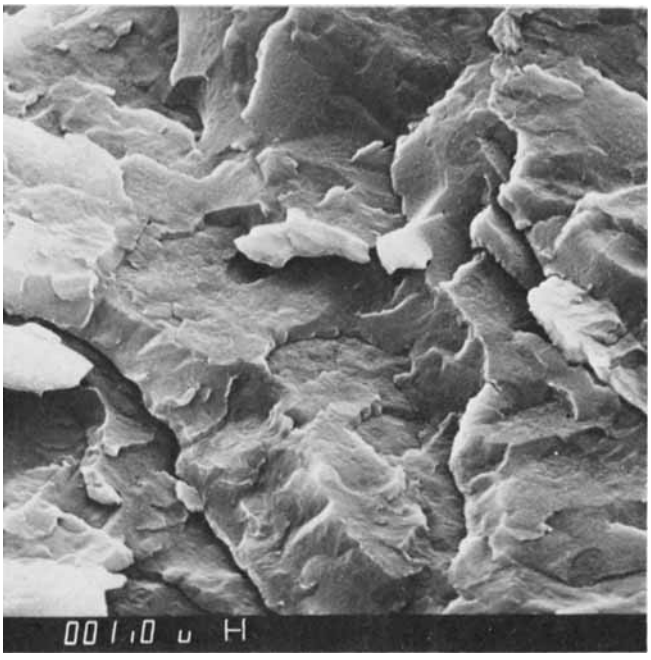

(a)

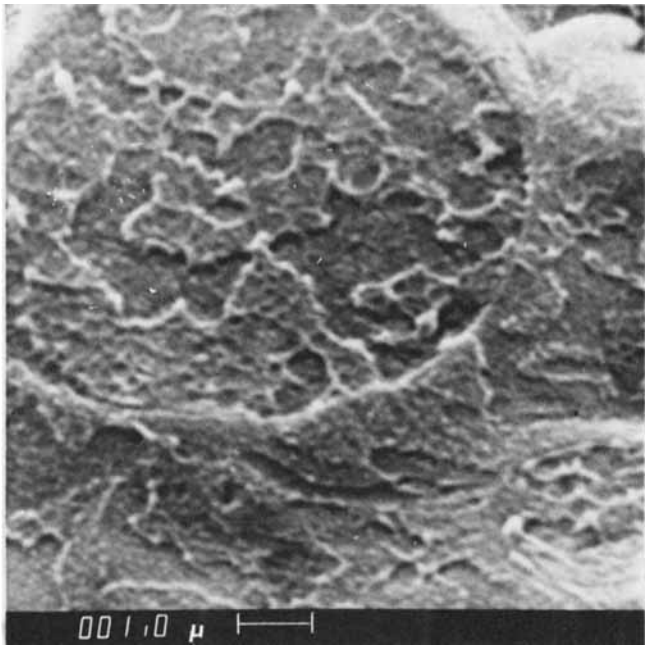

(b)

Fig. 12. Fracture surfaces of initially uncrazed HIPS specimens that have been strained to the failure. (Note that the fracture surfaces shown were those obtained by fracturing a remnant at liquid nitrogen temperatures.)

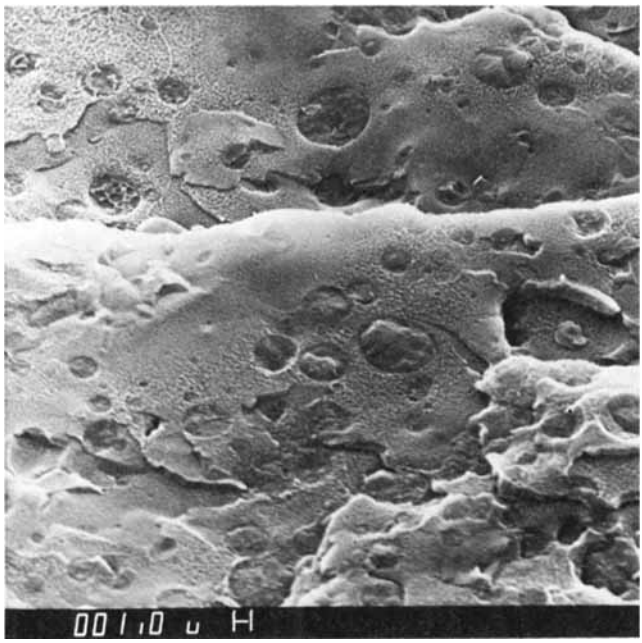

(a)

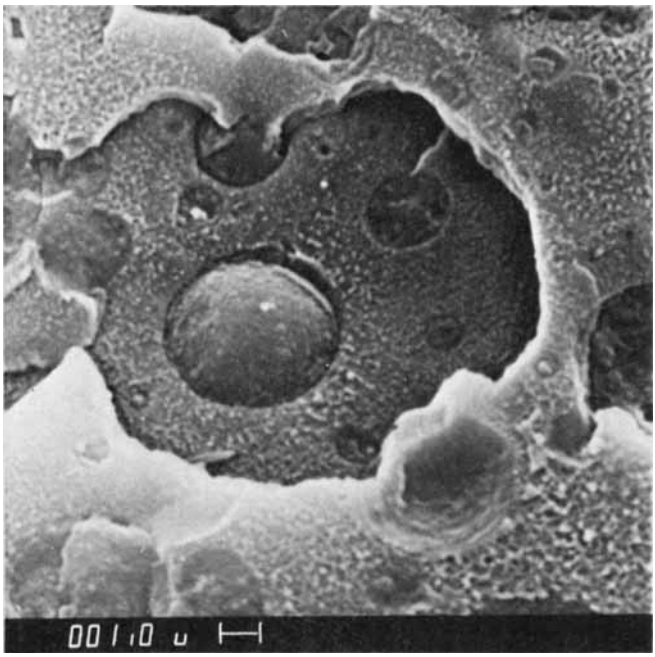

(b)

Fig. 13 (See caption on next page.)

diately on unloading[4] and therefore numerical correspondence will not be observed unless the time scales of the experiments are the same. Nevertheless, the initial approximately linear region of the tensile-strain curve for the uncrazed

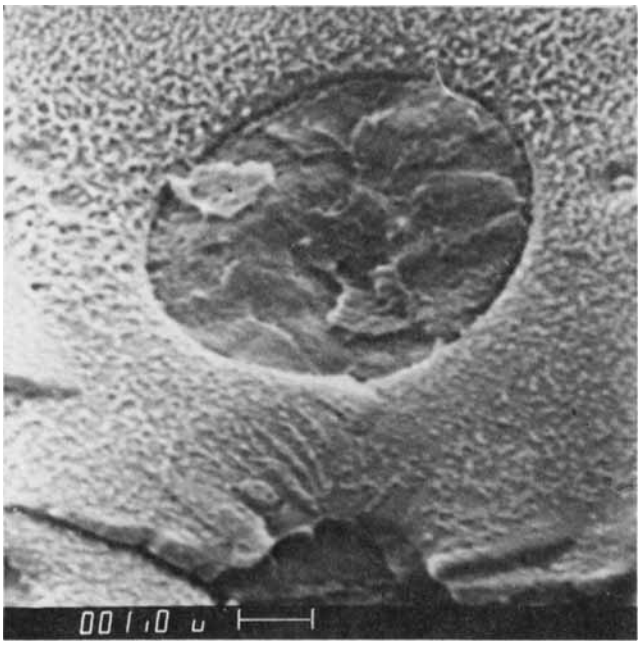

(c)

Fig. 13. Fracture surface of HIPS specimens subjected to 16,000 cycles of torsional oscillation at $\theta = 0.1$ rad and a tensile stress of σ_v 11 MPa at increasing magnification.

specimen can be seen to correspond to the amplitude independent region of the energy loss $\Delta E/\theta^2$ curves. On the linear region of the stress–strain curve, the polymer is known to behave as a linear visco-elastic solid at least over relatively short experimental times. This is to say, the ratio of stress to strain is a function of time alone and is independent of strain.

The onset of amplitude dependence at tensile stresses of $\sigma_v > 11.8$ MPa for the uncrazed specimen can be related to the region on the stress–strain curve where some "permanent" plastic strain begins. With the tensile test, this point is difficult to ascertain for a number of reasons. Firstly, the notion of there being a "permanent" strain is false, for, as mentioned already, dynamic recovery occurs on loading. Secondly, if one associates the presence of crazing with the initiation of "permanent" plastic deformation, then the first visual appearance of crazing can only be determined with some uncertainty. From the tensile test, crazes become visually obvious at stresses just below the yield stress σ_{Y1}. On the other hand, the beginning of amplitude dependence in the torsional oscillation experiments occurs at stress of $\sigma_v \simeq 11.8$ MPa, and this value corresponds approximately to the visual observation of crazes. It should be noted that the tensile component of the shear stress from the torsional oscillations is comparatively small compared to the applied tensile stress σ_v, so that the value of the combined stress σ_{max} to produce amplitude-dependent behavior (see Fig. 6) is only slightly higher at $\sigma_{max} = 11.9$ MPa at $\theta = 0.3$ rad.

After crazing has begun at stresses $\sigma_{max} > 11.9$ MPa, there still exist an amplitude-independent region up to angular deflections of $\theta \simeq 0.03$ rad. This be-

havior can be interpreted as a reaction of the partially opened crazes to a superimposed angular deflection which exceeds a critical value of θ before amplitude dependence occurs. Further evidence in support of this interpretation will be provided in the discussion of precrazed specimens.

For the precrazed specimens, the beginning of amplitude-dependent damping as a function of the applied tensile stress σ_v occurs in the same ranking order as the yield stress σ_{Y2}. That is, the tensile stress σ_v to produce a marked increase in amplitude-dependent damping occurs at 10.1 MPa for the 0° precrazed specimen, at 3.0 MPa for the 45° precrazed specimen, and at 1.3 MPa for the 90° precrazed specimen. It is noticeable, however, that for the precrazed specimens some amplitude dependence already exists at lower stresses at angular deflections above approximately $\theta = 0.03$ rad. For the 90° precrazed specimen, amplitude-dependent behavior remains constant above $\theta = 0.03$ rad until a tensile stress of $\sigma_v = 1.3$ MPa is obtained. Similar behavior is observed for the 45° and 0° precrazed specimens except that higher values of σ_v (respectively, $\sigma_v > 3.0$ and 10.1 MPa) are required to cause further increases in the energy loss. Apparently then, there exists, even at very low tensile stress levels σ_v, craze material which will react to the torsional oscillations at higher angular deflections and show nonlinear viscoelastic behavior.

The existence of amplitude-dependent behavior suggests that a form of plastic deformation begins at a maximum stress greater than a critical value σ^c_{max}. To understand this mechanism, it will be helpful to consider an alternative view of the test condition by referring again to the tensile stress–strain results. For example, if the 90° precrazed specimen is stressed to $\sigma_v = 5$ MPa, then the state of the crazed specimen will correspond to a position on the stress-strain graph (Figure 1), between σ_{Y2} and σ_D. At this position, the specimen is then subjected to an superimposed oscillating angular deflection. If amplitude dependent behavior is observed at particular values of $\sigma_{max} > \sigma^c_{max}$, then a mechanism must exist to allow continual energy absorption, for it has been shown that the energy loss $\Delta E/\theta^2$ curves are reproducible at least for tests with a cycle number less than approx. 1000 (see later discussion on fatigue). Two possible mechanisms to explain the behavior can be postulated.

Firstly, the oscillating shear stress may induce a shear strain in the craze that reverses in direction. This would suggest a craze structure that could be likened to a vertical array of cards—the oscillating shear stress acting to produce sliding, first in one direction, then a forced reversal in the opposite direction.

The second possible mechanism involves a partial recovery of the induced shear strain in each cycle. It has been shown[4] that if craze structures are unloaded, a process of recovery will occur. If the recovery time during oscillations is assumed to be approximately half the period of oscillation (i.e. 0.5 sec), then it would be expected from examination of Bucknall's[4] data on yield recovery that recovery may occur to the extent of approximately 10% of the initial yield stress.

The increase in the level of the energy loss $\Delta E/\theta^2$ curves as the stress σ_v is increased can be associated with two related phenomena. For the 90° precrazed specimen, the increase in stress σ_v above 1.3 MPa will, as stated previously, mean that shear stress oscillations are occurring about points on the stress–strain curve between σ_{Y2} and σ_D. Moving up the slope between these points implies, from previous work,[12–14] that existing crazes are opening. More craze material is then subjected to shear stress, and therefore a higher energy loss $\Delta E/\theta^2$ is recorded.

The other phenomenon is associated with the effect of strain rate. The initially uncrazed material suffered crazing during the damping experiment and visual examination suggested that the craze density was low. All precrazed specimens were strained at a medium cross-head speed (50 mm per min) and exhibited a considerably higher craze density. Thus, the energy loss $\Delta E/\theta^2$ will be correspondingly larger as the craze density increases with increased initial strain rates.

Most of the results indicated that the 45° precrazed specimen simply lies between the two extremes of behavior of the 0° and 90° precrazed specimens. The critical maximum stress σ^c_{max} for amplitude-dependent damping, the yield stress σ_{Y2}, and the shear modulus have intermediate values, but it is noticeable that amplitude-dependent damping begins at much lower values of θ.

The 0° precrazed specimen behaved in a rather similar manner to the initially uncrazed specimen. The presence of crazes in the parallel direction only lowered the craze initiation stress from 11.9 MPa to 10.1 MPa, but facilitated craze growth as indicated by the larger damping values. Similar results were obtained from the tensile tests, where, except for a slightly lower yield stress, the results are identical to that of the uncrazed specimen. Visual observation of the crazing of glassy polymers by Spurr and Niegisch[15] showed that stressing a specimen at right angles to existing crazes results in most new crazes being initiated in the undamaged matrix, with only relatively few crazes initiating from old crazes. The new crazes were found to be capable of growing to large widths and passing through the old crazes without deviation. It is apparent, therefore, that the presence of a craze structure containing voids and partially orientated chains cannot produce stress conditions suitable for the generation and growth of crazes at 90° to the original crazes.

A common feature with the energy loss $\Delta E/\theta^2$ results is that curves generally return to zero slope, indicating a corresponding return to amplitude-independent behavior and that no further plastic deformation of the craze material is occurring. This behavior may be due either to the fact that recovery is limited to a set strain or, alternatively, to a limit being placed on the extent of the deformation of the craze. It is known that the thickness of a craze may be determined by the size of rubber particles, but it is difficult to comprehend that this would place a limit on the deformation of a craze in, say, the 90° precrazed specimen loaded to relatively low tensile stresses.

The fatigue results indicate that repeated cycling has the effect of increasing the energy loss $\Delta E/\theta^2$ after the critical strain amplitude of $\theta = 0.03$ rad has been exceeded. Also, it is apparent that an induction period is required ($n > 4000$ cycles) before the energy loss becomes significant. The similarity between these results and the curves in Figures 5–7 suggests that repeated cycling may simply have the effect of increasing the total craze content.

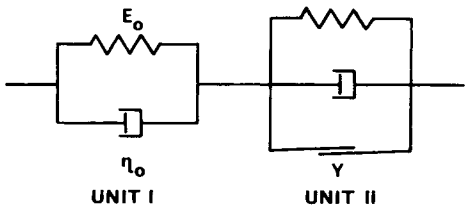

Fig. 14. Analogue model of the viscoplastic behavior of crazed polymer.

It is clear that once crazing has commenced in a polymer, the material can no longer be considered homogeneous, and indeed it is helpful to regard it as a composite material in which the cross-sectional areas of the components will change as further crazes are initiated. An analogue model can be constructed (Fig. 14) to describe the behavior.

At temperatures $T \ll T_g$ (polystyrene) and for experiments with relatively short times of loading, the unit I can be represented adequately by a spring E_0 and dashpot η_0. It is the viscoelastic energy loss from this unit that provides the amplitude-independent baseline behavior, as observed in Figure 7 at low angles of deflection. Unit II will characterize the behavior of the craze material from σ_{Y2} to σ_D. It contas a spring and dashpot to provide the features of time-dependent recovery and a plastic element Y that provides a yield stress.

An initially uncrazed specimen of HIPS will deform according to unit I until the first crazes are initiated and then unit II must be added. Continued straining at the stress σ_D will mean that more glassy material (unit I) is converted to crazed material (unit II), and therefore, as shown previously, the cross-sectional area of glass will decrease and the nominal area of craze material increase.

The presence of the sliding element will provide amplitude-dependent damping above a particular yield stress level. Justification for the incorporation of the plastic element is also seen from creep[1] experiments on crazed HIPS where the behavior is decidedly nonlinear.

However, it could be argued that the element Y should contain a maximum boundary limit and/or a strain-hardening function. It is known that crazes reach a maximum thickness that is probably dictated by the size of the rubber particle. Also from examination of the stress–strain behavior of the craze itself,[13,14] it appears that following a strain-softening inflection in the curve, considerable strain hardening occurs as σ_D is approached.

The support of the Australian Research Grants Commission through Grant No. F69/17226 to D. R. G. Williams is gratefully acknowledged.

References

1. C. B. Bucknall, *J. Mater. Sci.*, **7**, 1443 (1972).
2. S. Rabinowitz and P. Beardmore, *Crit. Rev. Macromol. Sci.*, **1**, 1 (1972).
3. R. P. Kambour, General Electric Co., Report No. 72CRD285, 1972.
4. C. B. Bucknall, D. Clayton, and W. Keast, *J. Mater. Sci.*, **8**, 514 (1973).
5. D. G. Legrand, *J. Appl. Polym. Sci.*, **16**, 1367 (1972).
6. C. Zener, *J. Appl. Phys.*, **18**, 1022 (1947).
7. H. Bartesch and D. R. G. Williams, *J. Phys. E:* Sci. Instrum., **10**, 416 (1977).
8. J. Hoare and D. Hull, *Phil. Mag.*, 443 (1971).
9. J. A. Sauer, J. Marin, and C. C. Hsiao, *J. Appl. Phys.*, **21**, 1071 (1949).
10. J. Stabenow and F. Haaf, *Angew. Macromol. Chem.*, **29/30**, 1 (1973).
11. B. J. Lazan, *Damping of Materials and Members in Structural Mechanics*, Pergamon, Oxford, 1968.
12. C. B. Bucknall, *J. Mater. Sci.*, **4**, 214 (1969).
13. R. P. Kambour, *Polym. Eng. Sci.*, **8**, 281 (1968).
14. R. P. Kambour and D. Kopp, *J. Polym. Sci. A-2*, **7**, 183 (1969).
15. O. K. Spurr and W. D. Niegisch, *J. Appl. Polym. Sci.*, **6**, 585 (1962).
16. J. A. Manson and R. W. Hertzberg, *J. Polym. Sci. A-2*, **11**, 2483 (1973).
17. C. B. Bucknall, *Brit. Plast.*, **40**, 84 (1967).

Received October 29, 1976
Revised December 13, 1976